
Proceedings Paper:
Ofir, R, Markovic, U, Aristidou, P et al. (2018) Droop vs. virtual inertia: Comparison from the perspective of converter operation mode. In: Proceedings of 2018 IEEE International Energy Conference (ENERGYCON 2018). ENERGYCON 2018: IEEE International Energy Conference, 03-07 Jun 2018, Limassol, Cyprus. IEEE, pp. 108-113. ISBN: 978-1-5386-3669-5.

https://doi.org/10.1109/ENERGYCON.2018.8398752

Droop vs. Virtual Inertia: Comparison from the Perspective of Converter Operation Mode

Ron Ofir*, Uros Markovic*, Petros Aristidou§, Gabriela Hug*
* EEH - Power Systems Laboratory, ETH Zurich, Physikstrasse 3, 8092 Zurich, Switzerland
§ School of Electronic and Electrical Engineering, University of Leeds, Leeds LS2 9JT, UK
Emails: ofirr@student.ethz.ch, {markovic, hug}@eeh.ee.ethz.ch, p.aristidou@leeds.ac.uk

***Abstract*—Virtual Inertia Emulation (VIE) and traditional Active Power Droop Control (APDC) are among the most common approaches for regulating the active power output of inverter-based generators. Furthermore, it has been shown that, under certain conditions, these two methods can be equivalent. However, neither those studies, nor the analyses of different dynamical properties between the two control schemes, have investigated the impact of the converter operation mode. This paper explores the subject by investigating the two control approaches under such conditions, and determining when this assumption does not hold. Using time-domain simulations with a detailed Voltage Source Converter model, we compare VIE and APDC qualitatively and reformulate the respective conditions for equivalence.**

***Index Terms*—voltage source converter (VSC), grid-forming, grid following, virtual inertia emulation (VIE), frequency droop**

I. Introduction

The penetration of Renewable Energy Sources (RESs) in present power systems is reaching an all-time high. As this type of generation is mostly interfaced to the grid via Voltage Source Converters (VSCs), we are currently facing large transmission grids being increasingly based on Power Electronic (PE) devices. Due to their significantly different physical properties when compared to traditional synchronous generator-based grids, it is necessary to develop appropriate control schemes for such systems. As part of a VSC control architecture, the Active Power Controller (APC) is used to adjust the frequency of the VSC output voltage, such that the active power injected by the converter meets a provided setpoint.

Two of the most common APC designs in the power systems community are Active Power Droop Control (APDC) and Virtual Inertia Emulation (VIE). APDC implements a linear relationship between frequency and active power balance, similar to the speed droop used in regulating synchronous machine governors [1]. Recent research on VSC control primarily focuses on microgrid operation, with concepts such as the reverse or opposite droop [2], virtual impedance [3] and adaptive droop [4], in order to resolve the challenges of resistive low-voltage lines and potential power coupling.

This project has received funding from the *European Union's Horizon 2020 research and innovation programme* under grant agreement No 691800. This paper reflects only the authors' views and the European Commission is not responsible for any use that may be made of the information it contains.

Similar to APDC, VIE is also inspired by traditional power systems, and aims to reproduce the grid-friendly dynamical properties of Synchronous Machines (SMs) in VSCs [5]–[10]. While different approaches exist in the literature, essentially they all rely on an internal mathematical model of a SM, which is used to determine the voltage or current reference signals for the converter. The internal model could be fully detailed, including the stator, damper and field windings, as well as the mechanical aspects of the machine, and supplying both voltage magnitude and frequency reference signals. An alternative approach would be to model only the rotational inertia by including the swing equation in the control scheme, thus using it to determine the frequency reference signal alone [6].

Although conceptually different from the APDC, a VIE approach also incorporates a droop-like scheme, imposed on the frequency deviation from a predefined steady-state value. It has been shown in this context that the two approaches are mathematically equivalent under certain conditions [11]. Mainly, the condition for equivalence is that the frequency and active power setpoints of the controllers are time-invariant. However, this highly depends on the system state, as well as the VSC mode of operation. The active power setpoint is usually determined via a higher-level control (AGC), and is manipulated during system operation in order to facilitate network stability. Additionally, the frequency setpoint might be constant or time-varying, depending on whether the VSC is operated as grid-forming or grid-following. This classification can have various meaning, depending on the type of application and control perspective [12]–[14].

In the context of the APC in an inverter-based transmission system, a grid-forming VSC is capable of establishing the grid frequency without the presence of a SM. On the other hand, a grid-following VSC measures the frequency and aligns its voltage accordingly, often using a synchronization unit such as a Phase-Locked Loop (PLL). Therefore, both setpoints might not be constant subject to how the VSC is operated, and it is reasonable to assume that APDC and VIE would result in different system dynamics. In [15], the authors provide a detailed dynamic comparison of the two control schemes based on small-signal analysis, focusing on the effect of system parameters on the small-signal model and the influence of time delays on the controller's performance. Similarly to [11],

the converter operation mode is not taken into account in the comparison.

The main distinction of VIE approach compared to the standard APDC is the inclusion of rotational inertia. On the one hand, an attempt to reproduce the behaviour of an actual SM could lead to a larger inertia constant than necessary, thus oversizing the required energy storage and increasing the cost of such a controller [16]. On the other hand, choosing a very low inertia constant reduces the total apparent inertia in the system and therefore compromises its stability [17]. This problem is also addressed in our study.

The contribution of this work is two-fold. First, we revisit the mathematical equivalence between APDC and VIE, and present the distinctions from the perspective of converter operation mode using a state-of-the-art VSC model. Second, we show that by introducing a damping torque equivalent into the swing equation of VIE, the inertia constant can be decreased while preserving the system stability.

The remainder of the paper is structured as follows. In Section II, a mathematical comparison of APDC and VIE control is presented. Section III describes the VSC model developed in this work. Section IV compares the transient response of the two controllers using time-domain simulations. Finally, Section V discusses the outlook of the study and concludes the paper.

II. APDC vs. VIE: A Comparative Analysis

A. Active Power Droop Control

APDC is a well-established control scheme for regulating the active power output of parallel converters, replicating the traditional primary frequency control of a SM. By appropriately adjusting the individual droop factors, it enables VSCs to share the load in proportion to their power rating using only local measurements. In this work, we focus on an inverter-based transmission system, assuming a full decoupling of active power and frequency from reactive power and voltage, which leads to the standard droop characteristic

$$\omega = \omega^* + D_p(p^* - \tilde{p}) \tag{1}$$

where ω^* and p^* are the frequency and active power setpoints, ω is the VSC output frequency, $\tilde{p}$ is the filtered active power measurement, and D_p is the droop slope.

Filtering of the power measurement is done via a first-order Low-Pass Filter (LPF)

$$\tilde{p} = \frac{\omega_c}{\omega_c + s} p \tag{2}$$

with the cutoff frequency ω_c and measured power p. As the whole APDC is done in per-unit system, the computed frequency is multiplied with the base value ω_b, and integrated in order to compute the respective phase angle θ. The resulting control scheme is shown in Fig. 1a.

B. Virtual Inertia Emulation

An alternative control approach to reproduce the stabilizing effects of SMs is by virtually emulating the missing (in VSC generators) rotational inertia. Several different implementations of such control architecture have been presented in the literature, defined as: synchronous VSC [10], virtual SM [6], virtual synchronous generator [7], [8], synchronous converter [9] and VISMA [5]. While the presented concepts differ in the level of detail of SM dynamics, as well as the role in VSC control scheme, they all incorporate an explicit formulation of the swing equation; described in the per-unit system as

$$2H\dot{\omega} = \frac{p^* - p}{\omega} - K_d(\omega - \omega^*) \tag{3}$$

with H and K_d denoting the inertia and damping constants, respectively. In order to simplify the comparison with the traditional APDC, VIE is implemented in closed loop within the APC, as depicted in Fig. 1b. For similar reasons, no filtering of the active power measurements has been included.

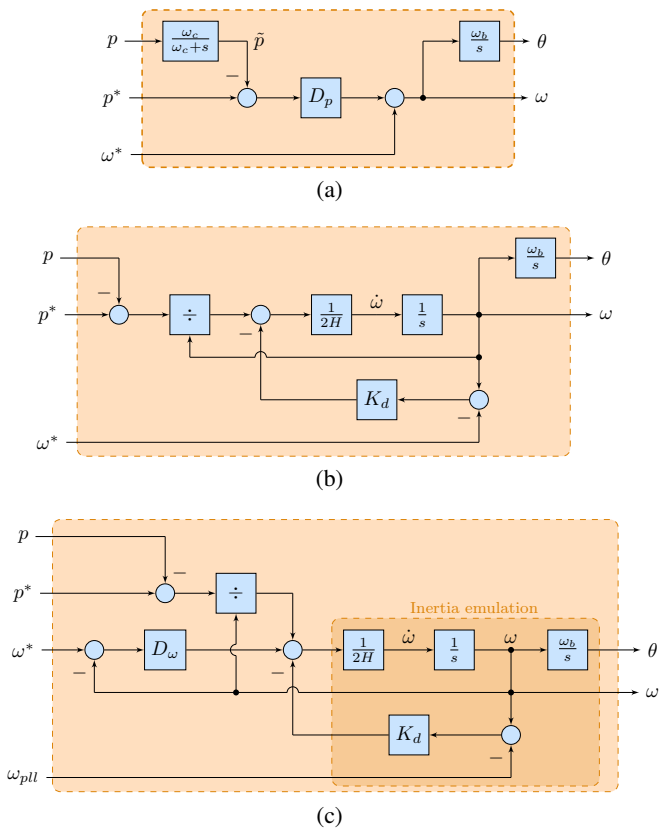

Fig. 1: Block diagrams of different APC implementation: (a) APDC; (b) VIE; (c) VIE with inclusion of the frequency droop.

C. Mathematical Equivalence

By analyzing the mathematical formulations of APDC in (1) and VIE in (3), we observe that both approaches use droop characteristics. However, in the first case it is imposed onto the power mismatch between the setpoint and measurement, while in the VIE approach, frequency deviation is used. As suggested by previous studies [11], [18], the two APC architectures can be proven mathematically equivalent under certain steady-state

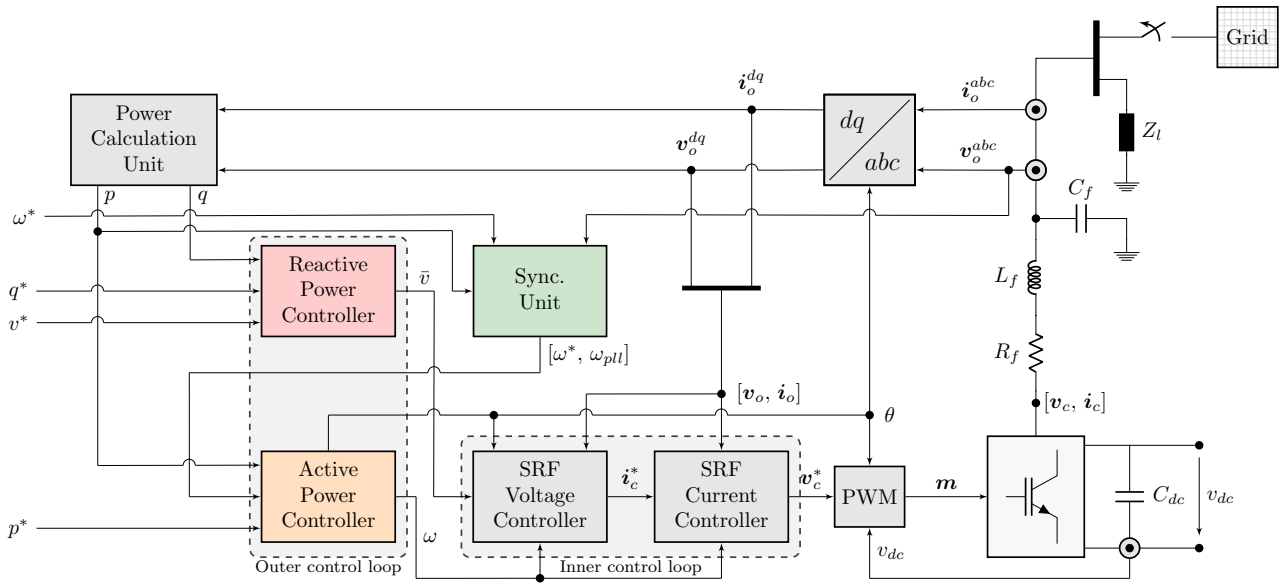

Fig. 2: Investigated system configuration and VSC control structure.

conditions. This can be proven by including the LPF transfer function in (1) and comparing it with (3):

$$\frac{1}{\omega_c D_p} s \cdot \omega = \frac{1}{D_p}(\omega^* - \omega) + p^* - p + \\ + \underbrace{\frac{1}{\omega_c D_p} s \cdot \omega^*}_{\sigma_\omega} + \underbrace{\frac{1}{\omega_c} s \cdot p^*}_{\sigma_p} \tag{4}$$

Assuming that $\omega \approx 1\,\text{p.u.}$ and $\sigma_\omega = \sigma_p = 0$, the following correlation between the parameters of (3) and (4) can be established:

$$H = \frac{1}{2\omega_c D_p} \quad , \quad K_d = \frac{1}{D_p} \tag{5}$$

enabling a computation of an equivalent VIE controller based on the parametrization of the analogous APDC, i.e. the LPF cutoff frequency and droop slope. Hence, several conditions for equivalence can be defined: (i) small frequency deviations around the nominal value; (ii) constant frequency setpoint input; and (iii) constant active power setpoint input. The fulfillment of these conditions is highly dependent on the VSC operation mode, as well as the power system itself, and will be investigated in detail throughout this study.

D. Converter Operation Mode

As previously described, from the perspective of the APC one can define two modes of operation, grid-forming and grid-following, which differentiate by the nature of frequency setpoint input ω^*. While this variation is quite straightforward in the case of an APDC, it can have a more complex physical interpretation in the VIE scenario. Let us examine the swing equation corresponding to a SM participating in primary frequency control:

$$2H\dot{\omega} = \frac{p^* - p}{\omega} - \underbrace{D_\omega(\omega - \omega^*)}_{\text{Droop}} - \underbrace{K_d(\omega - \omega_{pll})}_{\text{Damping}} \tag{6}$$

with D_ω and K_d denoting the respective droop and damping gains. Note that the resulting equation is equivalent to introducing an explicit frequency droop term in (3). Depending on the converter operation mode, the VIE scheme includes only one of these two gains, i.e. D_ω in grid-forming and K_d in grid-following scenario. Furthermore, this suggests that using both inputs (ω^* and ω_{pll}) results in a control scheme that includes a droop characteristic for active power sharing, as well as a damping torque emulation which improves the overall system stability. Note that such APC, depicted in Fig. 1c, is always considered grid forming, as the damping term converges to zero in steady-state.

III. VSC Control Scheme

An overview of the studied VSC model is shown in Fig. 2, consisting of an ideal DC voltage source, interfaced through a DC/AC converter, RLC filter and a transformer to the grid. The control scheme contains an outer loop which uses the voltage and current measurements to compute the reference voltage magnitude and frequency by means of active and reactive power controllers. These reference signals are then passed through the inner control loop consisting of cascaded voltage and current controllers. The model also includes a grid synchronization unit that provides the frequency setpoint for the outer control loop, either as a constant value or a PLL measurement.

A. Reactive Power Controller

Similar to the APC, the Reactive Power Controller (RPC) adjusts the magnitude of the VSC output voltage to meet a provided reactive power setpoint. In this work, we assume that the RPC regulates the voltage around a constant setpoint v^* via a droop-based controller described by

$$\bar{v} = v^* + D_q\,(q^* - \tilde{q}) \tag{7}$$

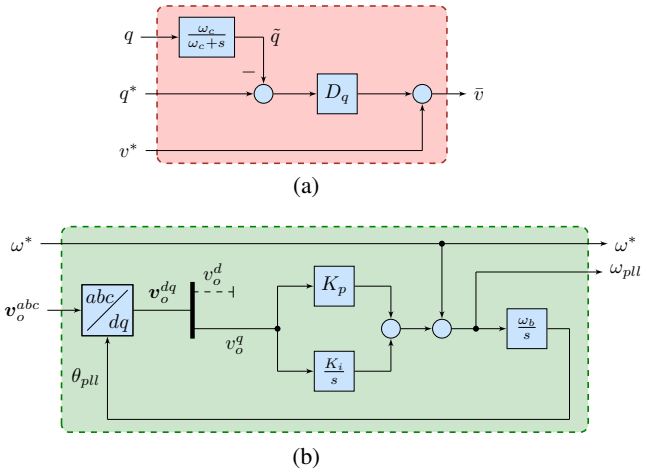

Fig. 3: Remaining outer loop control blocks of the VSC control scheme: (a) Reactive power controller; (b) Phase-Locked Loop.

where $\bar{v}$ is the computed voltage reference, D_q is the droop gain, and q^* and $\tilde{q}$ are the setpoint and filtered measurement of reactive power. A block diagram of the controller is presented in Fig. 3a.

B. Synchronization Unit

The synchronization unit provides adequate frequency setpoint to the outer control loop. In the case of a grid-forming VSC this is just a constant reference, whereas a PLL is used for the purposes of a grid-following VSC. A Type-2 PLL operating in a Synchronous Reference Frame (SRF) has been implemented in this study, as described in [19] and shown in Fig. 3b. It is based on the (dq)-transformation of a balanced three-phase voltage signal $\boldsymbol{v}_o^{abc}$ with a magnitude v_m and a frequency ω

$$\boldsymbol{v}_o^{dq} = \boldsymbol{T}_p \boldsymbol{T}_c \boldsymbol{v}_o^{abc} = v_m \begin{bmatrix} \cos(\theta - \theta_{pll}) \\ \sin(\theta - \theta_{pll}) \end{bmatrix} \tag{8}$$

with $\theta = \int \omega dt$ and $\theta_{pll} = \int \omega_{pll} dt$, as well as $\boldsymbol{T}_c$ and $\boldsymbol{T}_p$ denoting the Clarke and Park transformation matrices. The synchronization is achieved by initially aligning the d-axis of SRF with the voltage vector, hence diminishing the q-component. Reasonably assuming $v_m \approx 1$, this would equate to $\sin(\theta - \theta_{pll}) \approx 0$ in (8), i.e. $\theta \approx \theta_{pll}$. The PLL is implemented as a PI controller of the phase angle difference, treating it as an error signal and driving it to zero.

C. Inner Control Loop and Modulation

Once the desired voltage magnitude and frequency are determined by the outer control, the inner control regulates the VSC output, such that the voltage after the filter meets the reference signal. This is done using two cascaded loops, the first regulating the voltage and the second regulating the current. This sequential implementation enforces the saturation of the converter output current in a controllable manner [6]. A state-of-the-art SRF control scheme has been implemented in this study, as discussed in [14]. Following the inner control loop is a modulation block, which calculates the modulation index for the VSC switching by applying the inverse (dq)-transform and averaging over the DC-side voltage.

IV. Results

In this section, the proposed APCs are qualitatively compared under different operation modes, as well as different system conditions. The averaged converter model presented in the previous section was implemented in MATLAB Simulink with the use of SimPowerSystems toolbox for modeling the external components (network lines, loads, etc.). The nominal parameters of the VSC are as follows: AC voltage $V_n = 320\,\text{kV}$; DC voltage $V_{dc} = 640\,\text{kV}$; active power $P_n = 1\,\text{GW}$; power factor $\cos\varphi_n = 0.95$; frequency $f_n = 50\,\text{Hz}$; active power droop $D_p = 0.02\,\text{p.u.}$ and reactive power droop $D_q = 0.001\,\text{p.u.}$ Each of the aforementioned conditions for equivalence from Section II is individually investigated, with the main conclusions subsequently drawn.

A. Large Frequency Deviation

In order to study the sensitivity of the proposed equivalence to frequencies differing from $\omega = 1\,\text{p.u.}$, a VSC is connected to a constant resistive load of $P_L = 500\,\text{MW}$. The grid-forming operation mode is selected, i.e. the APC setpoints are kept constant, so that only the effect of frequency deviation is observed. This is simulated by increasing the load power in a step fashion 100 ms after the simulation start, as shown in Fig. 4. The step change of $\Delta P_L = 100\,\text{MW}$ results in frequency deviation of $\Delta f \approx 0.05\,\text{Hz}$, which does not have any impact on the equivalence between the two control schemes, since the responses are identical. This is expected since all setpoints remain constant and the maximal frequency deviation is smaller than $0.001\,\text{p.u.}$, hence justifying all three aforementioned conditions for equivalence. A drastically higher load change of 450 MW leads to a proportionally higher deviation from nominal frequency of $\Delta f \approx 0.4\,\text{Hz}$. Under such circumstances, a negligible deviation between the two APCs is observed, indicating that the frequency deviation does not impose any restrictions on the droop-VIE equivalence.

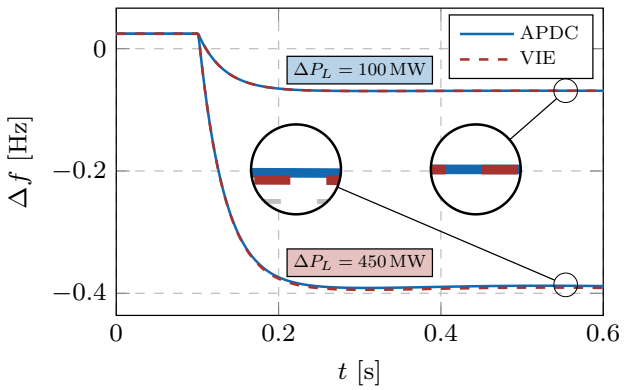

Fig. 4: VSC frequency response to a load step change.

B. Change in Active Power Setpoint

This subsection addresses the assumption of a constant active power setpoint and its impact on the performance of the controllers. Since an islanded mode of operation prevents the VSC from following its active power setpoint, in this test case the converter is connected to a strong grid with a short circuit ratio of 20. Additionally, the VSC is operated as a grid-forming, to make sure only the active power setpoint derivative influences the response. A step increase of $\Delta P^* = 0.1$ p.u. is introduced 100 ms after the simulation start, and the behavior of VSC frequency and active power output is depicted in Fig. 5. The droop controller exhibits a sharp rise in frequency, replicating the familiar fast transients of low inertia systems. This is expected as the LPF is only applied to the power measurement, directly translating the step in active power setpoint into a step in VSC frequency. On the contrary, VIE slows down the frequency dynamics due to an explicit inertia emulation term. Furthermore, the active power output is also improved, with the higher damping and a decrease in overshoot of roughly 50 %. It can be concluded that VIE outperforms traditional droop control in case of a time-variant active power setpoint, and the suggested equivalence does not stand.

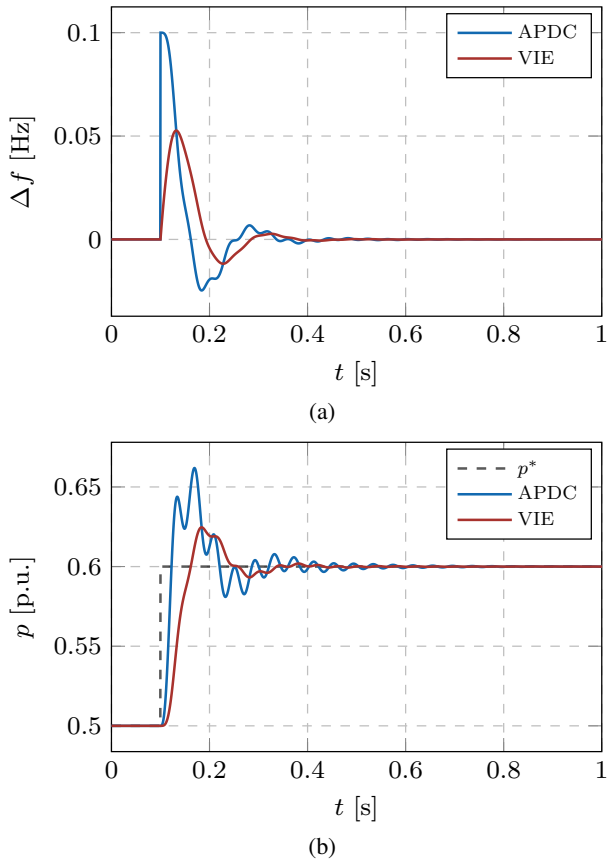

Fig. 5: VSC response to a step change in active power setpoint: (a) Variation of the computed frequency; (b) Variation of the active power output.

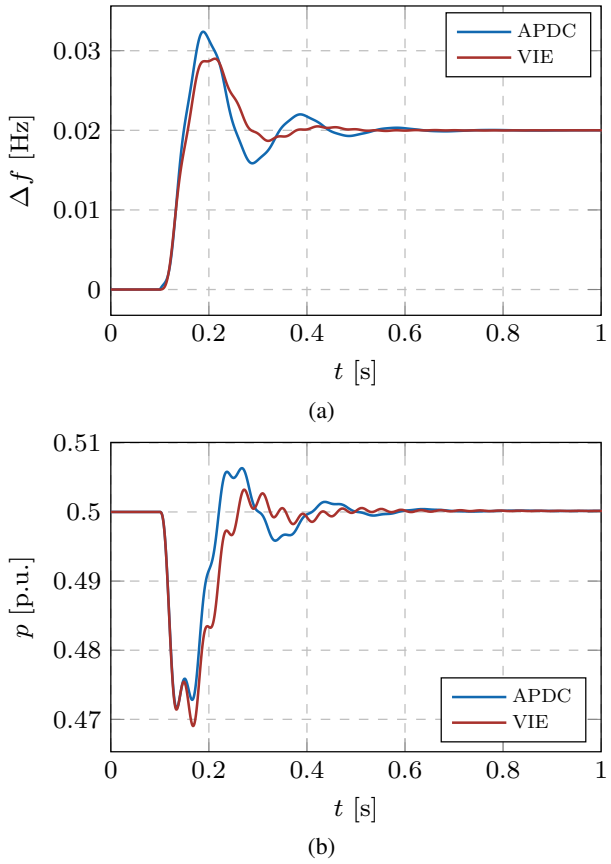

Fig. 6: VSC response to a step change in grid frequency: (a) Variation of the computed frequency; (b) Variation of the active power output.

C. Change in Frequency Setpoint

The aim of this case study is to analyze the effect of a time-varying frequency setpoint on the performance of droop and VIE controllers. Therefore, it implies operating the VSC in a grid-following mode, with the reference coming from a PLL measurement. Since such configuration has no standalone capabilities, the converter is again connected to a strong grid, and the active power setpoint is kept constant. We observe a transient response to a step increase of $\Delta f = 20$ mHz in grid frequency occurring 100 ms after the simulation start, shown in Fig. 6. Due to the inherent PLL dynamics, a step in grid frequency is not directly transferred to the APC, but rather as a gradual increase in estimated frequency. Hence, the distinction between the two control schemes is not as significant as in the previous test case. The VSC power output exhibits similar performance, whereas the frequency response of a VIE has slightly lower overshoot and better damping.

D. Reduction of Virtual Inertia Requirement

The study in Section IV-B has shown the biggest improvements of VIE compared to the droop. Since it was operated in a grid-forming mode, the control scheme only incorporated a frequency droop term from (6). In order to reduce the level of required virtual inertia, we investigate in this subsection the

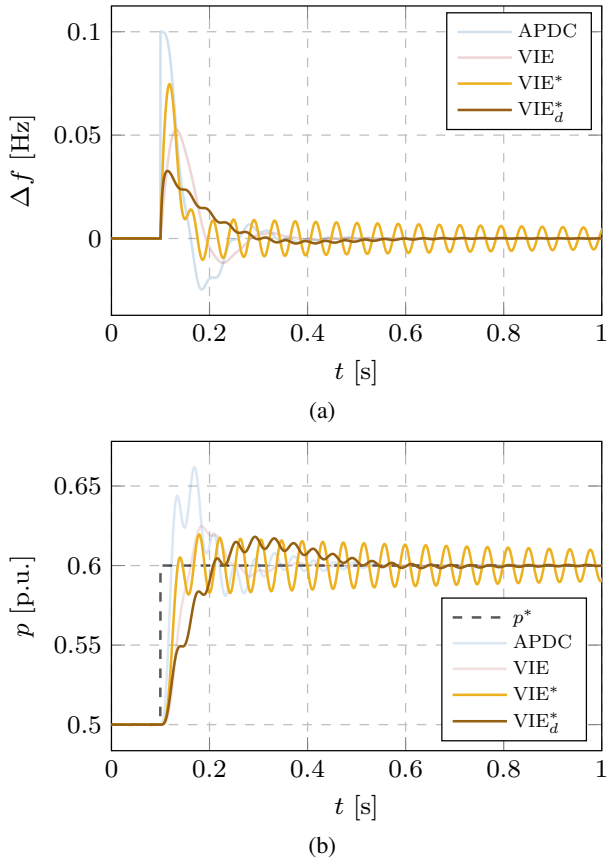

Fig. 7: VSC response to a step change in active power setpoint: (a) Variation of the computed frequency; (b) Variation of the active power output.

potential of simultaneously introducing the damping torque, similar to a VIE controller depicted in Fig. 1c and suggested in Section II-D. First, a VIE controller with the inertia constant reduced to a third of its original value is used, denoted with VIE*, and the active power setpoint change is simulated. This results in an undamped system, with increased active power and frequency excursions, as shown in Fig. 7. The results of this simulation are overlaid on top of the results presented in Section IV-B. To mitigate the destabilizing effects of reduced inertia, a damping term is now incorporated in a grid-forming VIE model, which is equivalent to damping constant K_d in (6). The results of this simulation are denoted VIE$^*_d$. It can be seen that in addition to restoring system stability, this improved controller outperforms the original VIE architecture with a larger inertia constant in terms of overshoot, while providing comparable damping characteristics. Also note that using reduced inertia constant, with or without an additional damping term, the overshoot in both frequency and power output responses is smaller than for the droop APC scenario.

V. Conclusion

In this paper, a qualitative comparison of APDC and VIE was presented. The mathematical equivalence of the two approaches was readdressed to highlight the effects of the respective converter operation mode. A physical interpretation of grid-forming and grid-following concepts was introduced, from the perspective of APC. Subsequently, a detailed model of VSC was described including the outer and inner loops, as well as the synchronization unit. Finally, using time-domain simulations, APDC and VIE were compared in different scenarios and the distinctions in dynamic response were elaborated. We have shown that VIE offers overall lower overshoot and better damping compared to the droop, while providing slower frequency transients. Furthermore, it has been proven that the inclusion of the damping torque in the emulated SM model enables significant decrease of the required inertia constant, while offering comparable stability performance.

References

[1] M. C. Chandorkar, D. M. Divan, and R. Adapa, "Control of parallel connected inverters in standalone ac supply systems," *IEEE Transactions on Industry Applications*, vol. 29, no. 1, pp. 136–143, Jan. 1993.

[2] A. Engler, "Applicability of droops in low voltage grids," *International Journal of Distributed Energy Resources*, vol. 1, no. 1, pp. 1–6, 2005.

[3] J. He and Y. W. Li, "Analysis, design, and implementation of virtual impedance for power electronics interfaced distributed generation," *IEEE Transactions on Industry Applications*, vol. 47, no. 6, pp. 2525–2538, Nov 2011.

[4] J. C. Vasquez, J. M. Guerrero, A. Luna, P. Rodriguez, and R. Teodorescu, "Adaptive droop control applied to voltage-source inverters operating in grid-connected and islanded modes," *IEEE Transactions on Industrial Electronics*, vol. 56, no. 10, pp. 4088–4096, Oct 2009.

[5] H. P. Beck and R. Hesse, "Virtual synchronous machine," in *2007 9th International Conference on Electrical Power Quality and Utilisation*, Oct 2007.

[6] S. D'Arco and J. A. Suul, "Virtual synchronous machines - classification of implementations and analysis of equivalence to droop controllers for microgrids," in *2013 IEEE Grenoble Conference*, June 2013.

[7] J. Driesen and K. Visscher, "Virtual synchronous generators," in *2008 IEEE Power and Energy Society General Meeting - Conversion and Delivery of Electrical Energy in the 21st Century*, July 2008.

[8] T. V. Van, K. Visscher, J. Diaz, V. Karapanos, A. Woyte, M. Albu, J. Bozelie, T. Loix, and D. Federenciuc, "Virtual synchronous generator: An element of future grids," in *2010 IEEE PES Innovative Smart Grid Technologies Conference Europe (ISGT Europe)*, Oct 2010.

[9] S. M. Ashabani and Y. A. R. I. Mohamed, "General interface for power management of micro-grids using nonlinear cooperative droop control," *IEEE Transactions on Power Systems*, vol. 28, no. 3, pp. 2929–2941, Aug 2013.

[10] M. Ashabani and Y. A. R. I. Mohamed, "Novel comprehensive control framework for incorporating vscs to smart power grids using bidirectional synchronous-vsc," *IEEE Transactions on Power Systems*, vol. 29, no. 2, pp. 943–957, March 2014.

[11] S. D'Arco, J. A. Suul, and O. B. Fosso, "Small-signal modelling and parametric sensitivity of a virtual synchronous machine," in *2014 Power Systems Computation Conference*, Aug 2014.

[12] A. Tabesh and R. Iravani, "Multivariable dynamic model and robust control of a voltage-source converter for power system applications," *IEEE Transactions on Power Delivery*, vol. 24, no. 1, pp. 462–471, Jan 2009.

[13] Q.-C. Zhong and T. Hornik, *Control of power inverters in renewable energy and smart grid integration*. John Wiley & Sons, 2012, vol. 97.

[14] J. Rocabert, A. Luna, F. Blaabjerg, and P. Rodrguez, "Control of power converters in ac microgrids," *IEEE Transactions on Power Electronics*, vol. 27, no. 11, pp. 4734–4749, Nov 2012.

[15] J. Liu, Y. Miura, and T. Ise, "Comparison of dynamic characteristics between virtual synchronous generator and droop control in inverter-based distributed generators," *IEEE Transactions on Power Electronics*, vol. 31, no. 5, pp. 3600–3611, May 2016.

[16] M. P. N. van Wesenbeeck, S. W. H. de Haan, P. Varela, and K. Visscher, "Grid tied converter with virtual kinetic storage," in *2009 IEEE Bucharest PowerTech*, June 2009.

[17] A. Ulbig, T. S. Borsche, and G. Andersson, "Impact of Low Rotational Inertia on Power System Stability and Operation," *ArXiv e-prints*, Dec. 2013.

[18] N. Soni, S. Doolla, and M. C. Chandorkar, "Inertia design methods for islanded microgrids having static and rotating energy sources," *IEEE Transactions on Industry Applications*, vol. 52, no. 6, pp. 5165–5174, Nov 2016.

[19] S.-K. Chung, "A phase tracking system for three phase utility interface inverters," *IEEE Transactions on Power Electronics*, vol. 15, no. 3, pp. 431–438, May 2000.